Progress In Electromagnetics Research M, Vol. 29, 165–179, 2013

ON THE ROTATIONALLY-CYLINDRICAL MODEL OF THE HUMAN BODY EXPOSED TO ELF ELECTRIC FIELD

Abdelmalek Laissaoui[1], Bachir Nekhoul[1], Kamal Kerroum[2], Khalil El Khamlichi Drissi[2], and Dragan Poljak[3, *]

[1]LAMEL Laboratory, University of Jijel, BP 98 Ouled Aissa, Jijel 18000, Algeria

[2]Clermont Université, Université Blaise Pascal, BP 10448, F-63000 Clermont Ferrand CNRS, UMR 6602, Institut Pascal, Aubière F-63177, France

[3]Faculty of Electrical Engineering, Mechanical Engineering an dNaval Architecture, University of Split, R. Boskovica 32, Split HR-21000, Croatia

Abstract—The paper presents an assessment of human exposure to extremely-low-frequency (ELF) electric field generated by a power line using the rotationally-cylindrical body model. The formulation is based on the Laplace type continuity equation. The induced current density in the three-dimensional (3D) model human body is obtained by solving the Laplace equation via the Finite element method (FEM). The main objective is to highlight some parameters influencing the distribution of the induced current density, such as the ohmic contact between the feet and the soil due to the soles of the shoes, and the electrical parameters of the soil. Furthermore, the influence of internal organs (the human model) to the induced current density distribution. The human body is represented by a homogeneous model and also by an inhomogeneous model composed of several organs namely brain, heart, lungs, liver and intestines, whose shapes were spheroid. The proposed model has been validated through comparison to either the experimental results or the theoretical results available in literature being computed by the aid of a homogeneous body model.

Received 28 January 2013, Accepted 25 February 2013, Scheduled 26 February 2013

* Corresponding author: Dragan Poljak (dpoljak@fesb.hr).

1. INTRODUCTION

Exposure to electromagnetic fields is not a new phenomenon. However, during the 20th century, environmental exposure to electromagnetic fields generated by human activity has increased steadily, in conjunction with the electric power demand and the continued progress of the technology. Thus, human being is exposed to a complex set of electric and magnetic fields of low intensity, both at home and at workplace, whose sources range from the generation and transmission of electricity, domestic appliances and industrial equipment, to telecommunications and broadcasting.

To address this societal constraint, electrical engineering community, as well as researchers from other disciplines involved are requested to provide a clear answer. To achieve this goal, it is crucial to provide researchers from Life Sciences with appropriate elements and measures to quantify the phenomena occurring in the human body due to exposure to electromagnetic fields. This analysis should be available prior to any biomedical study to enable the assessment of potential biological effects which should result in setting up the appropriate standards for the optimization of corresponding protection systems.

Computational bioelectromagnetics can be classified into two groups:

- low frequency exposures in which electric and magnetic fields are decoupled,
- high frequency exposures in which the energy absorption from electromagnetic radiation is dominant effect [1].

At extremely low frequencies, the effects of the electric field and magnetic field of the human body can be studied independently of one another. There are two scenarios for human exposure to low frequency fields, as follows:

- High voltage/low current systems — the case of power lines HV and UHV in which the effect of the electric field is predominant over the magnetic field. The coupling between the electric field and the human body causes the axial current density inside the body.
- Low voltage/high current systems — the case with the most of electrical appliances, either domestic or industrial ones in which the magnetic field considered to be predominant. The coupling between the magnetic field and the human body is the cause of circular (closed loops) current density inside the human body.

Note, that according to ICNIRP guidelines from 1998 [2] the current density was a main parameter for the estimation of extremely low

frequency exposure effects, while the new ICNIRP guidelines from 2010 [3] propose the induced electric field instead of the induced current. However, there is a substantial amount of results for the current density in the relevant literature for the comparison purposes, e.g., [4–13]. Several methods have been used to calculate the current density induced in the human body due to exposure to low frequency fields, such as the Finite Difference Time Domain (FDTD) [4, 5] the Finite Element Method (FEM) [6–8]; the Boundary Element Method (BEM) [9–10]; the impedance method [11] or the Transmission Line (TL) model [12].

Within the framework of the Finite Element Method (FEM) it is possible to use higher order elements and consequently avoid very fine meshes, thus making it rather useful for applications with complex shapes and highly irregular geometries.

Electromagnetic phenomena represented by related partial differential equations are being solved by using different FEM formulations. For example in [12] FEM formulations involving the induced currents are discussed.

The present work deals with an inhomogeneous rotationally-symmetrical model of the human body. To quantify the induced current density inside the human body exposed to uniform electric field, the FEM formulation based on the scalar electric potential (Electro-Quasi-Static formulation) is applied. The analysis is undertaken via COMSOL Multiphyisics software [14].

First, the influence of the soil and the ohmic contact due to the soles of the shoes on the induced current density distribution is analyzed. The sensitivity of the induced current density in the body when conductivities of the five internal organs (the brain, heart, lungs, liver and intestines) are taken into account is studied.

2. FORMULATION

Figure 1 shows the axisymmetrical and homogeneous geometry of the human body being used by Japanese team [6, 7]. The human body model is composed from nine parts (Dimensions are given in centimetres).

When considering the human exposure to high voltage and low intensity systems, such as overhead power lines, the electric field is dominant. The formulation is based on the quasi-static version of the continuity equation [6]:

$$-\nabla \cdot [(\sigma + j\omega\varepsilon_0\varepsilon_r)\nabla\varphi] = 0 \tag{1}$$

where ω is the frequency of the incident field, ε_0 the free space

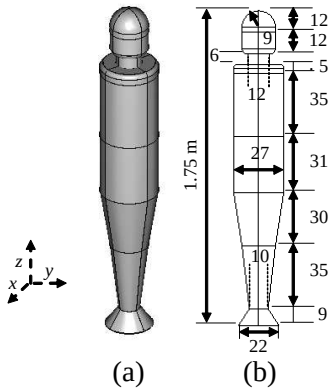

Figure 1. (a) The three-dimensional human body model, (b) basic dimensions.

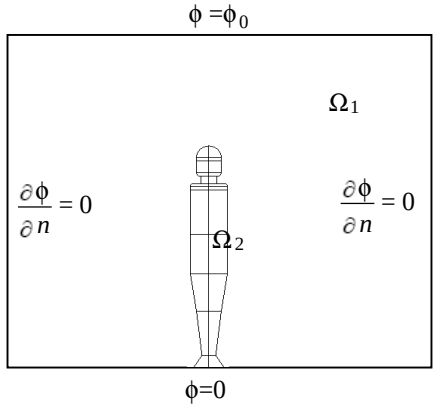

Figure 2. Calculation domain with the prescribed boundary conditions.

permittivity, σ and ε_r are the conductivity and relative permittivity of the material and φ is the electric scalar potential.

The partial differential Equation (1) is imposed on the human body and the surrounding air, respectively.

Knowing the scalar potential along the body, the induced current density can be obtained from the Ohm's Law of Equation (2):

$$\vec{J} = (\sigma + j\omega\varepsilon)\nabla\phi \tag{2}$$

where σ is the conductivity of the human tissue and ε the permittivity given by $\varepsilon = \varepsilon_r\varepsilon_0$.

The electric field E can be computed from the gradient of the scalar potential gradient φ:

$$\vec{E} = -\nabla\phi \tag{3}$$

3. THE AIR-BODY INTERFACE CONDITION

A calculation domain with the corresponding boundary conditions is shown in Figure 2.

The sources of the electric field are expressed through the Dirichlet boundary conditions; the scalar potential must be specified at the location of the power lines and soil level. Neumann conditions may be used to truncating the calculation domain by truncation, i.e., the normal component of electric field is zero on the other two faces of the cube, Figure 2.

Furthermore, Figure 2 shows the crosscut section of the model where domain Ω_1 is the region of air having two parameters: the permittivity ε_0 and the permeability μ_0. Domain Ω_2 is the region of the human body having three parameters: the relative permittivity ε, the permeability μ, and the conductivity of the body σ.

In the case of the internal boundaries between two domains Ω_1 and Ω_2, the continuity equation is expressed as follows [16]:

$$\vec{n} \cdot \left(\vec{J}_1 - \vec{J}_2 \right) = 0 \quad \text{(Condition of current continuity)} \tag{4}$$

or as presented in [16]:

$$j\omega\varepsilon_0 \vec{n} \cdot \vec{E}_{air} = (\sigma + j\omega\varepsilon)\vec{n} \cdot \vec{E}_{tissue} \tag{5}$$

Note that the relationship (5) which expresses the continuity of the normal component of the current at the interface of two domains.

If the human organs are not taken into account one deals with the homogeneous domain, i.e., on the surface of the human body the lines of the current density current are tangential, consequently the normal component of the current is zero, same as in the air due to the displacement current being neglected.

On the other hand, if one accounts for the human organs the domain of interest is inhomogeneous.

In this case the domain is represented by a primary domain (the body) and in its interior by subdomains which represent the organs of the human.

When the human organs are included within the formulation, several domains of interest are considered as each organ is represented by a domain with related parameters. In this case in each domain the partial differential equation given by quasi-static formulation (1) is solved. In this case the condition of continuity (4) is implemented between each organ and the surrounding environment (body) and between the human body and the air.

4. COMPUTATIONAL EXAMPLES

4.1. Electric Field Exposure

In the proposed model the conductivity and permittivity of the human body are assumed to be: $\sigma = 0.5\,\mathrm{S{\cdot}m^{-1}}$ and $\varepsilon_r = 10^7$ with $\mu = \mu_0$ (Note that in low frequency range biological tissues are mostly diamagnetic).

The body with a height of $L = 1.75\,\mathrm{m}$ is placed in direct contact (barefoot) with the soil, as depicted in Figure 3, and exposed to a

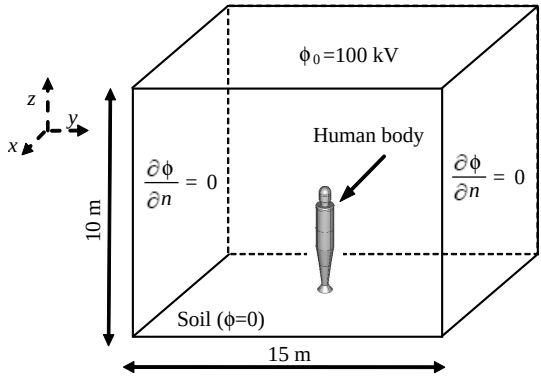

Figure 3. The human body model in a uniform electric field.

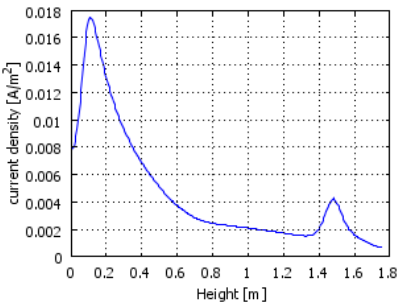

Figure 4. Axial current density distribution.

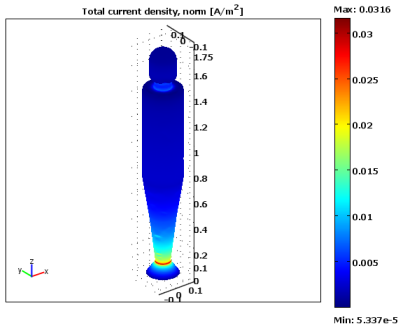

Figure 5. Current density induced on the surface of the human body.

uniform vertical electric field $E_z = 10\,\mathrm{kV{\cdot}m^{-1}}$, while the height of the power line (height of the domain) was set 10 m.

Figures 4 and 5 show the induced current density along the axis and surface of the body, respectively.

It could be noticed that the current density values are higher in the neck and ankles due to their relatively smaller cross-sectional areas. The results calculated in this paper via FEM are compared to the results obtained by other either theoretical or experimental methods and listed in Table 1. The FEM results are shown to be in a satisfactory agreement with those achieved by Poljak et al. [10] using the Boundary Element Method (BEM) and with experimental results of Chiba et al. [8].

Table 1. Comparison between the BEM, FEM and experimental results expressed in [mA/m^2].

Part of the body	FEM	BEM [10]	Experimental [8]
Neck	4.25	4.52	4.66
Pelvis	2.09	2.32	2.25
Ankles	17.5	18.91	18.66

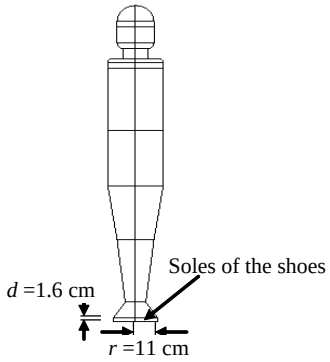

Figure 6. The human body model including the soles of shoes.

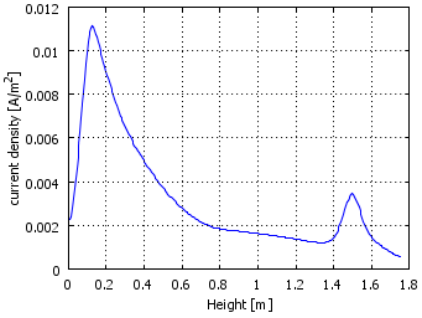

Figure 7. Axial current density distribution.

4.2. Influence of the Soles of the Shoes

It is worth noting that so far a perfect contact between the body and the soil has been assumed. However, in majority of real scenarios there exists an ohmic contact between the feet and the soil, particularly due to the influence of the soles of shoes. This contact is generally represented by an equivalent capacitor, e.g., [8, 11, 15]. In the model proposed in this work the soles are modeled by a volume of height $d = 1.6\,\text{cm}$ (height of the sole) and radius $r = 11\,\text{cm}$, as indicated in Figure 6, characterized by a relative permittivity $\varepsilon_r = 3$.

Keeping the same dimensions of the air box and the value of the incident electric field of the preceding case the current density induced along the axis and surface of the body, respectively is presented in Figures 7 and 8.

It could be clearly observed from the obtained results that, due to the influence of the shoes, values of the induced current density tend to decrease, particularly in the feet and ankles as shown in Figure 7.

4.3. Influence of Soil

The next step is to study the influence of the soil parameters to the behaviour of the current density induced in the human body.

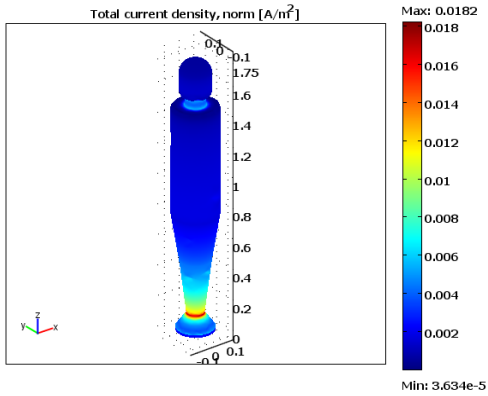

Figure 8. Current density induced on the surface of the human body.

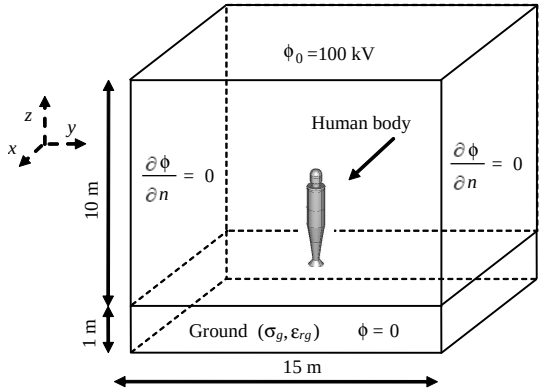

Figure 9. The model of the human body exposed to a uniform electric field in the presence of soil.

To illustrate the influence of the conductivity and relative permittivity of the soil, some representative values of the conductivity and relative permittivity of the soil available in literature [16], i.e., $\sigma_g = 1000$; 0.2; 0.5; 10^{-2}; 10^{-3} (S·m^{-1}), $\varepsilon_{rg} = 5$, 10, 30 is used. The soil is modeled as a homogeneous volume as shown in Figure 9.

The results presented in Figures 10 and 11 show that the induced current density varies slightly at the interface between the human body and the soil, but the maximum and average values remain similar. Moreover, when the soil conductivity is higher than the body conductivity, all curves are observed to converge rapidly towards the curve corresponding to $\sigma_g = 1000\,\mathrm{S{\cdot}m^{-1}}$.

The results of shown in Figures 12 and 13 show that the current

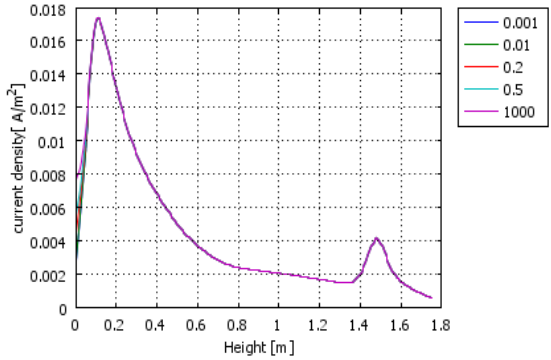

Figure 10. Induced current density inside the body.

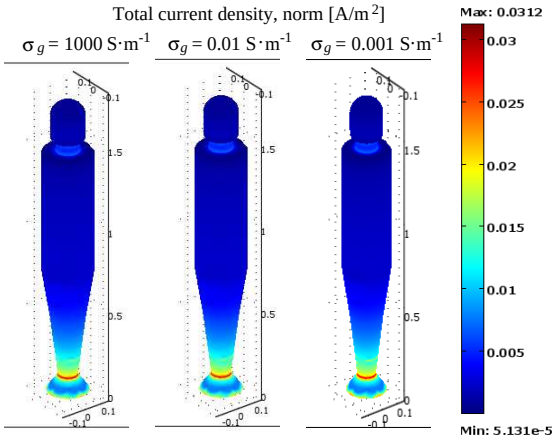

Figure 11. Induced current density on the surface of the human body for different soil conductivities (ε_{rg} =10).

induced in the body does not vary appreciably with the permittivity of the soil.

It can be observed that the soil parameters do not seem to have any significant influence on the current density induced in the human body. This is consistent with results available in the literature [17].

4.4. Influence of Organs

To estimate the effect on the induced current distribution inside the human body due to the presence of organs (organs of different conductivity), the body model having taken into account five organ (brain, heart, lungs, liver and intestines) has been assembled.

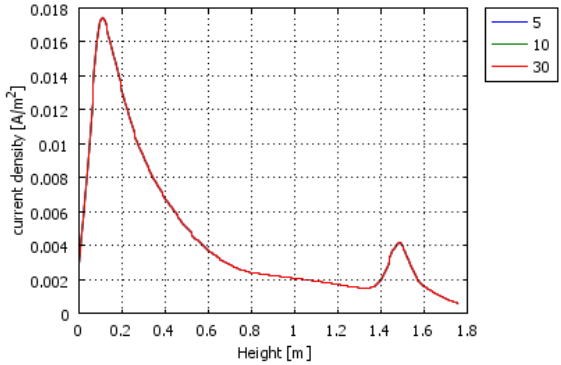

Figure 12. Induced current density inside the body.

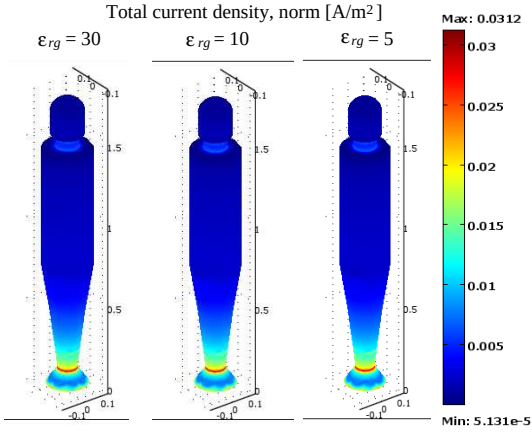

Figure 13. Induced current density on the surface of the human body for different relative permittivity of the soil ($\sigma_g = 0.01\,\mathrm{S{\cdot}m^{-1}}$).

The organs are represented by spheroidal shapes, as depicted in Figure 14 [18].

The conductivities, the dimensions and the coordinates of the various organs are obtained from the literature [18, 19] and listed in Tables 2 and 3, respectively. Magnitude and frequency of electric field was 10 kV/m and 60 Hz.

Figures 15 and 16 show the variation of the current density along the axis of the human body and on the surface of the latter, obtained by using the homogeneous and inhomogeneous representation of the body, respectively. To provide the comparison between the results the calculations were carried out for a conductivity of the order of $0.2\,\mathrm{S{\cdot}m^{-1}}$ in the case of the homogeneous model.

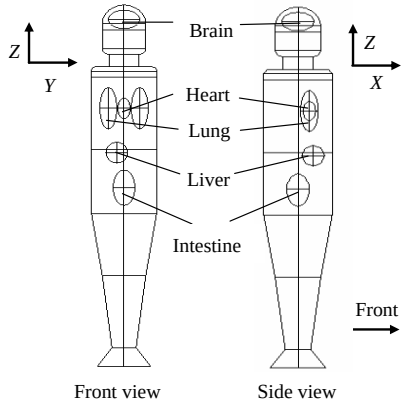

Figure 14. Human models with the organs included.

Table 2. Organ conductivity assigned to human models [18, 19] (Unit: $S \cdot m^{-1}$).

Organ	Homogeneous model	Inhomogeneous model
Brain	0.2	0.75
Heart	0.2	0.7
Lung	0.2	0.10
Liver	0.2	0.10
Intestines	0.2	0.03
Others	0.2	0.11

Table 3. Shape and coordinates of respective organs [19] (Unit: mm)

elements of prolate spheroid shape: (center coordinates x, y, z-elliptic radii, y, z)	
Brain	(0, 0, 1685, 65, 45)
Left Lung	(45, −65, 1250, 35, 100)
Right Lung	(45, 65, 1250, 35, 100)
Heart	(45, 0, 1250, 25, 50)
Liver	(60, −30, 1060, 45, 50)
Intestines	(0, 0, 900, 45, 85)

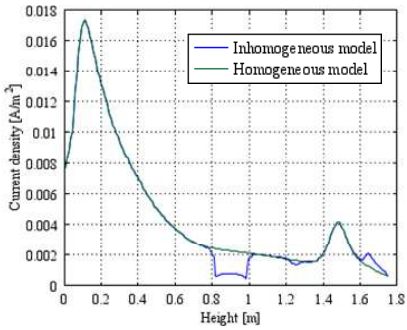

Figure 15. Induced current density inside the body ($x = 0$; $y = 0$).

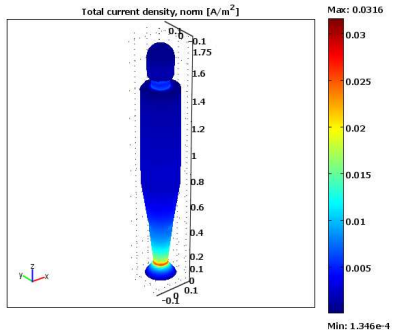

Figure 16. Induced current density on the surface of the human body.

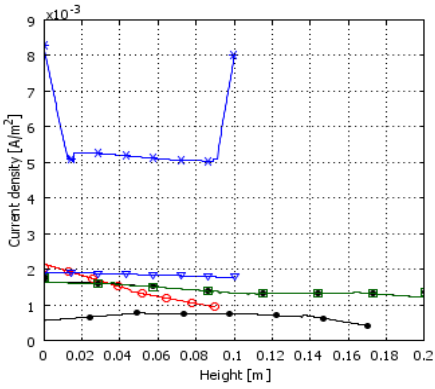

Figure 17. Induced current density in each organ.

Observing the results shown in Figure 15 following conclusions can be drawn:

- The induced current density in the feet and ankles does not differ for the two models;
- There is an increase of the current density in the brain and a decrease in the intestines when compared to the results obtained with the homogeneous model of the body. This is due to the difference in electrical conductivity which is high in the brain ($\sigma = 0.75\,\mathrm{S{\cdot}m^{-1}}$) and low in the intestines ($\sigma = 0.03\,\mathrm{S{\cdot}m^{-1}}$).

4.4.1. Comparison of Magnitudes of Induced Current Densities at Respective Organs

Figure 17 represents the variation of the induced current density in the different organs, traced along the respective axes of the organs (see Table 3 and Figure 14).

The maximum values of current density and electric field induced inside the different organs are given in Table 4.

Table 4. Induced electric field and current density.

Organ	Current density $J_{\max}$ [mA/m^2]	Electric field $E_{\max}$ [V/m]
Heart	8.665	0.0124
Brain	2.150	0.0029
Lung	1.770	0.0177
Liver	1.940	0.0194
Intestines	0.7932	0.0264

From the results presented in Figure 17 and Table 4 it can be concluded that the induced current density in the different organs is dependent on the conductivity and the dimensions (radius) of the organs.

5. CONCLUSION

In this paper, the finite element method (FEM) has been used to solve the electro-quasi-static (EQS) formulation aiming not only to characterize the current density induced in the human body due to electric field exposure at extremely low frequencies but also to clarify the influence of various parameters on the current density distribution. The conclusions that could be drawn are, as follows:

- In the homogeneous model of the human body the current density is observed to be marginally influenced by the electrical parameters of the soil. However, the wearing of shoes significantly contributes to a reduction of the induced current density level inside the body. The comparison of the calculated results with existing data available in the literature provided a validation of the proposed model to a certain extent.
- In the inhomogeneous model of the body, having taken into account electrical properties of five organs, the influence of the electrical conductivities and the dimensions of organs to the current density behaviour has been noticed.

REFERENCES

1. Gonzalez, C., A. Peratta, and D. Poljak, "Boundary element modelling of the human body when exposed to overhead power lines: Influence on conductivity variations," *17th International Conference on Software, Telecommunications & Computer Networks, SoftCOM 2009*, 1–5, Sep. 2009.
2. International Commission on Non-ionizing Radiation Protection, "Guidelines for limiting exposure to time-varying electric, magnetic and electromagnetic fields (up to 300 GHz)," *Health Physics*, Vol. 74, No. 4, 494–522, Apr. 1998.
3. International Commission on Non-ionizing Radiation Protection, "Guidelines for limiting exposure to time-varying electric and magnetic fields (1 Hz–100 kHz)," *Health Physics*, Vol. 99 No. 6, 818–836, Dec. 2010.
4. Stuchly, M. A. and T. W. Dawson, "Human organ and tissue induced currents by 60 Hz electric and magnetic fields," *Proceedings of 19th International Conference of IEEE, Engineering in Medicine and Biology Society*, Vol. 6, 2464–2467, Chicago, IL USA, Oct. 30–Nov. 2, 1997.
5. Kong, L.-Y., J. Wang, and W.-Y. Yin, "A novel dielectric conformal FDTD method for computing SAR distribution of the human body in a metallic cabin illuminated by an intentional electromagnetic pulse (IEMP)," *Progress In Electromagnetics Research*, Vol. 126, 355–373, 2012.
6. Chiba, A. and K. Isaka, "Analysis of current densities induced inside a human model by the two-step process method combining the surface-charge integral equation and the finite-element method," *Electronics and Communications in Japan, Part 2, Electronics*, Vol. 79, No. 4, 102–111, 1996.
7. Chiba, A. and K. Isaka, "Density distribution of currents induced inside the brain in the bead part of the human model exposed to power frequency electric field," *IEEE 11th Int. Symp. High Voltage Eng.*, Vol. 1, No. 467, 307–310, London, 1999.
8. Chiba, A., K. Isaka, Y. Yokoi, M. Nagata, M. Kitagav, and T. Matsuo, "Application of finite element method to analysis of induced current densities inside human model exposed to 60 Hz electric field," *IEEE Trans. Power Apparatus and Systems*, Vol. 103, No. 7, 1895–1902, 1984.
9. Poljak, D. and Y. Rashed, "The boundary element modelling of the human body exposed to the ELF electromagnetic fields," *Elsevier Engineering Analysis with Boundary Elements*, Vol. 26,

No. 10, 871–875, 2002.

10. Poljak, D., C. Gonzales, and A. Peratta, "Assessment of human exposure to extremely low frequency electric fields using different body models and the boundary element analysis," *18th ICECom International Conference on Applied Electromagnetics and Communications*, 109–112, 2005.
11. Deford, J. F. and O. P. Gandhi, "An impedance method to calculate currents induced in biological bodies exposed to quasi — Static electromagnetic fields," *IEEE Transactions on Electromagnetic Compatibility*, Vol. 27, No. 3, 168–173, 1985.
12. Mezoued, S., B. Nekhoul, D. Poljak, K. ElKhamlichi Drissi, and K. Kerroum, "Human exposure to transient electromagnetic fields using simplified body models," *Engineering Analysis with Boundary Elements*, Vol. 34, No. 1, 23–29, 2010.
13. Biro, O. and K. Preis, "On the use of the magnetic vector potential in the finite element analysis of three-dimensional eddy currents," *IEEE Transaction on Magnetics*, Vol. 25, No. 4, 3145–3159, 1989.
14. Comsol Version 3.5a, COMSOL Multiphysics Finite Elements Analysis Software, COMSOL, Stockholm, Sweden.
15. Furse, C. M. and O. P. Gandhi, "Calculation of electric fields and currents induced in a millimeter resolution human model at 60 Hz using the FDTD method," *Bioelectromagnetics*, Vol. 19, 293–299, 1998.
16. King, R. W. P., "A review of analytically determined electric fields and currents induced in the human body when exposed to 50–60-Hz electromagnetic fields," *IEEE Transactions on Antennas and Propagation*, Vol. 52, No. 5, 1186–1192, 2004.
17. Hoang, L. H., "Contribution à la modélisation tridimensionelle des interactions champ électromagnétique corps humain en basses fréquences," Thèse No. E.C.L.2007-32, École Centrale de Lyon, 2007.
18. Yamazaki, K., T. Kawamoto, H. Fujinami, and T. Shigemitsu, "Investigation of ELF magnetically induced current inside the human body: Development of estimation tools and effect of organ conductivity," *Electrical Engineering in Japan*, Vol. 134, No. 2, 1013–1020, 2001.
19. Min, S. W., E. S. Kim, and S. H. Myung, "Calculation and measurement of induced current density inside human body under 60 Hz ELF magnetic fields," *EMC 09*, Vol. 21S3-2, 185–188, Kyoto, 2009.